CHEMISTRY
A European Journal

A Journal of
ChemPubSoc Europe

Accepted Article

Title: Ullazine Donor-π bridge-Acceptor Organic Dyes for Dye-Sensitized Solar Cells

Authors: Yanbing Zhang, Hammad Cheema, Louis McNamara, Leigh Anna Hunt, Nathan Hammer, and Jared Heath Delcamp

To be cited as: *Chem. Eur. J.* 10.1002/chem.201800030

Link to VoR: http://dx.doi.org/10.1002/chem.201800030

Supported by
ACES

WILEY-VCH

10.1002/chem.201800030

WILEY-VCH

FULL PAPER

Ullazine Donor-π bridge-Acceptor Organic Dyes for Dye-Sensitized Solar Cells

Yanbing Zhang,[†] Hammad Cheema,[†] Louis McNamara, Leigh Anna Hunt, Nathan I. Hammer, Jared H. Delcamp*[a]

Abstract: A series of 4 ullazine-donor based donor-π bridge-acceptor (D-π-A) dyes have been synthesized and compared to a prior ullazine donor-acceptor (D-A) dye as well as a triphenylamine donor with an identical π-bridge and acceptor. The D-π-A ullazine series demonstrates an unusually uniform-in-intensity panchromatic UV-Vis absorption spectrum throughout the visible region. This is in part due to the introduction of strong high-energy bands through incorporation of the ullazine building block as shown by computational analysis. The dyes were characterized on TiO_2 films and in DSC devices. Performances of 5.6% power conversion efficiency were obtained with IPCE onsets reaching 800 nm.

Introduction

Dye-sensitized solar cells (DSCs) have attracted increasing attention since 1991 due to low manufacturing costs, affordable solar cell materials, easy integration into building materials and the potential to meet energy production needs.[1] DSCs operate through light absorption by a sensitizer or dye anchored to a semiconductor, electron transfer from the excited-state dye to the semiconductor, collection of the electron by a redox shuttle at a counter electrode after it has traveled an external circuit, and return of the electron to the oxidized dye by the redox shuttle. The sensitizer component of the DSC devices plays a critical role in controlling light absorption and subsequent electron transfers. Organic sensitizers based on the conjugated donor-π-acceptor (D-π-A) framework offer a modular synthesis, high molar extinction coefficient, and tunable molecular design which has furnished organic dyes outperforming precious metal containing sensitizer with power conversion efficiencies (PCEs) of over 13%.[2] Additional improvements to organic sensitizers are possible by extending the absorption range with precise control of the sensitizer energy levels. A key functionality needed for many D-π-A dye systems to extend their absorption spectrum is the donor building block.[3] Frequently, organic dyes do not have ground-state oxidation potentials well positioned for minimal energy loss as a result of the limited availability of stable, strong electron donating functionality.[4] Typically, phenyl amine organic molecular building blocks such as coumarin, indoline, triphenylamine, carbazole are employed as donors.[2a, 5] However, these donors often lack planarization of the nitrogen lone pair with the dye π-system, conjugation of all p-orbitals on the donor building block, and the ability to add additional electron donating groups in conjugation with the dye π-system.[3b] These inherent challenges have led to the extensive evaluation of various electron rich π-bridges to compensate for the lack of desired donor strength. The use of a planarized *peri*-fused nitrogen containing building blocks such as ullazine offers a potential solution to each of these challenges.

Ullazine is a 16 π-electron planar nitrogen containing *peri*-fused heterocyclic system which is isoelectronic with pyrene.[3a, 3c, 6] Ullazine is fully conjugated with a number of substitutable positions for modulating donor strength and tuning dye morphologies. Ullazine has a charge separated anionic 14 π-electron aromatic annulene resonance structure around the periphery which enhances the donation strength of the nitrogen lone pair by favoring charge separation (Figure 1). This charge-separated state can be used to promote intramolecular charge transfer (ICT) at lower energies. Additionally, upon ICT, an aromatic ring arises on ullazine in the excited-state. This proaromatic pyridinium ring serves to lower the energy necessary for ICT by aromatically stabilizing the excited-state.[3b, 3d, 7] These desirable attributes have been shown to shrink optical band by ~ 0.7 eV when compared with an analogous triarylamine donor based dye.[3c] Ullazine has also known to be stable during redox processes as is desirable within a solar cell device.[6g] Due to these properties, ullazine has recently attracted interest in donor-acceptor dyes and as a donor for porphyrin sensitizers in DSC devices.[3c, 6a] However, to date ullazine has only been evaluated once in metal-free donor-π bridge-acceptor sensitizers despite the potential for robust, panchromatic organic dyes which are desperately needed in DSCs.[6j]

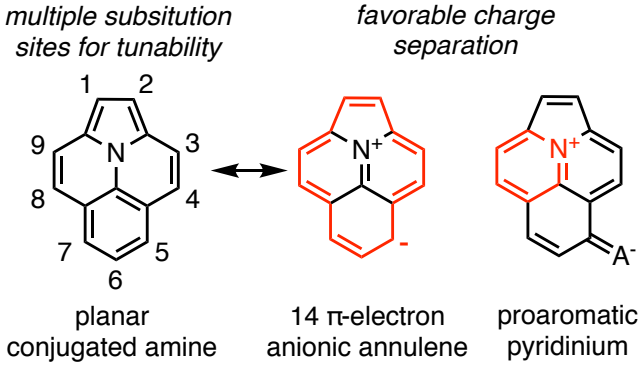

Figure 1. Ullazine building block with resonance structures drawn to illustrate favorable ICT.

[a] Yanbing Zhang,[†] Hammad Cheema,[†] Louis McNamara, Leigh Anna Hunt, Nathan I. Hammer, Jared H. Delcamp*.
Department of Chemistry and Biochemistry
University of Mississippi, University, MS 38677 (MS)
E-mail: delcamp@olemiss.edu

[†] Authors contributed equally.

Supporting information for this article is given via a link at the end of the document.

10.1002/chem.201800030

Results and Discussion

Given the promising known properties of ullazine, a series of novel D-π-A based ullazine dyes were targeted for synthesis (Figure 2). This series focused on the incorporation of two different aryl groups on ullazine with either a *para*-alkoxy group to maintain a highly electron rich donor (**YZ7** and **YZ12**) or di-*ortho*-alkoxy groups extending over the ullazine π-face to disrupt any potential π-stacking based aggregation (**YZ14** and **YZ15**). Given the two strongest donating positions (the 4 and 5 positions) of ullazine are ortho substituted, an alkyne was chosen to link the donor to the π-bridge in order to enable access to a fully planarized π-system conformation. The dyes with identical aryl substituents vary in position of an alkyne linking group either at the meta position relative to the nitrogen substituent on the fused benzene ring (5 position) or at the position adjacent to the aryl group (4 position). Cyclopentadithiophene (CPDT) was chosen as an electron rich π-bridge since DSC dyes typically have considerable energy losses due to lack of electrons with high enough potential energy in the ground state of the dye to reach ideal energetics. Additionally, CPDT is a well-established π-bridge in high efficiency DSCs which allows for a straight forward comparison of a ullazine-alkyne donor to common amine donors such as triphenylamines (TPAs).[8] All dyes utilize the ubiquitous cyanoacrylic acid acceptor.

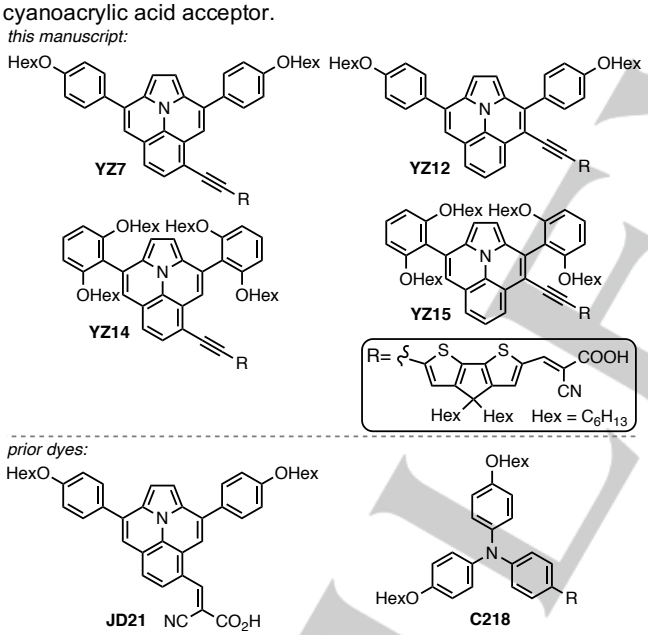

Figure 2. Structure of ullazine-based dyes **YZ7, YZ12, YZ14, YZ15,** and **JD21** as well as TPA dye **C218**.

The synthesis of **YZ7**, **YZ12**, **YZ14** and **YZ15** is briefly described here from known intermediates (Scheme 1). The ullazine heterocycle with two di-*ortho*-hexyloxyphenyl groups was synthesized similar to prior analogs.[3c] Briefly, the di-*ortho*-hexyloxyphenyl alkyne (**2b**) was synthesized from the corresponding aryl aldehyde (**1b**) via treatment with TMS-diazomethane and LDA in 91% yield. Alkyne **2b** was coupled to dibromophenyl pyrrole **3** via a Sonogashira reaction in 83% yield. $InCl_3$ catalyzed cyclization furnished parent ullazine **5b** in 29% yield. Formyl groups were installed via Vilsmeyer-Haack reaction to give the two desired isomers **6b** and **7b**, which were separated via silica gel chromatography and carried forward.[3c] The aldehydes **6a, 6b, 7a** and **7b** were subjected to modified Corey-Fuchs

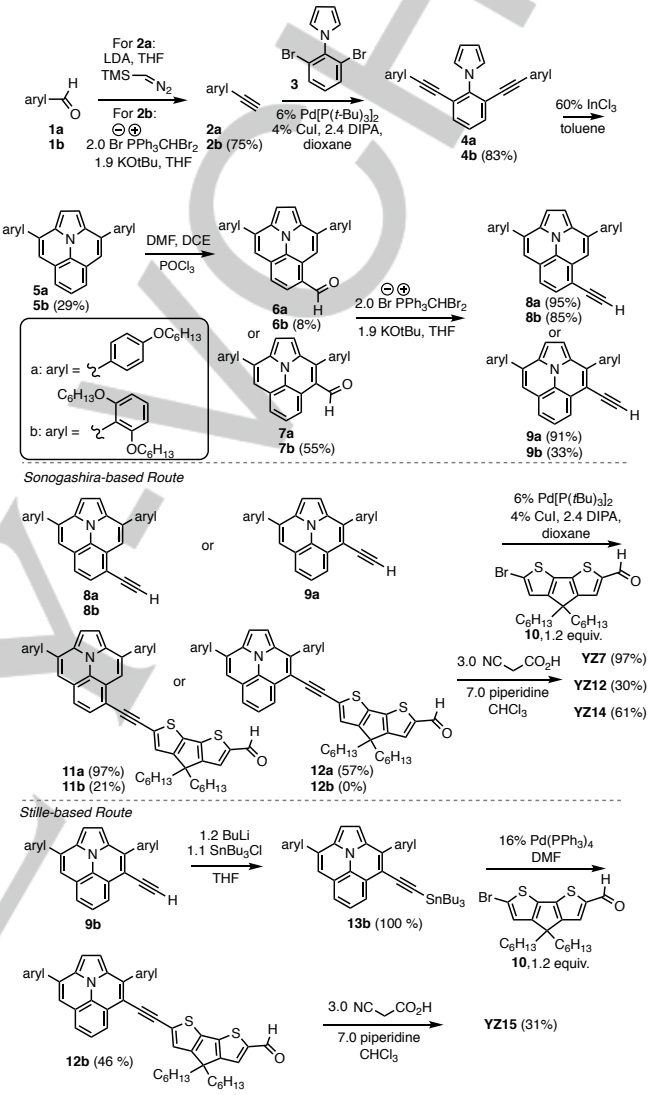

Scheme 1. Synthetic route to **YZ7**, **YZ12**, **YZ14** and **YZ15**. Yields are only listed for compounds which are novel to this manuscript.

reaction conditions to give desired alkynes **8a**, **8b**, **9a**, and **9b** in high yield except for derivative **9b** presumably due to sterics. For aldehyde precursors to final dyes **YZ7**, **YZ12** and **YZ14**, Sonogashira cross couplings with 6-bromo-4,4-dihexyl-4H-cyclopenta[2,1-b:3,4-b']dithiophene-2-carbaldehyde **10** and intermediates **8a**, **8b**, or **9a** were carried out in low to high yields. Alkyne **9b**, a precursor to **YZ15**, gave no desired product under similar conditions, thus an alternative alkyne-stannylation/Stille coupling route was used to furnish the desired aldehyde **12b** in 46% yield. Knoevenagel condensation on the resulting aldehydes (**11a**, **11b**, **12a**, or **12b**) furnished the desired dye series.

With the desired dyes in hand, the absorption properties of the **YZ** dyes were examined to determine the suitability of these

dyes in DSC devices and to better understand the effects of the ullazine-donor group on ICT. The ullazine-based dyes have a broad absorbance from 400-700 nm with high molar absorptivities of (26,000-29,000 $M^{-1}cm^{-1}$, Figure 3, Table 1). The absorption spectra of **YZ7-YZ15** exhibit an intense peak at around 535 nm, which is due to the HOMO-LUMO transition of the conjugated molecule (discussion below). The introduction of the alkyne-CPDT π-system to give a D-π-A structure lead to a red-shift of the absorption spectrum relative to D-A ullazine-cyanoacrylic acid dye **JD21** (Figure 2).[3c] Additionally, the D-π-A structure broadened the absorption spectrum relative to the simple D-A dye and led to the introduction of a strong high-energy absorption band. This high-energy transition band is unique to ullazine D-π-A CPDT bridged dyes as triphenylamine analogues such as **C218** only have a single strong absorption band in the visible region.[9] This is important as the introduction of high-energy bands in the absorption spectrum has been related to higher performing DSC devices due to a more uniform absorption of the solar spectrum.[10] The molar absorptivities of these high energy bands are comparable to that of the ICT low energy band ranging from about 15,000-30,000 $M^{-1}cm^{-1}$. Dyes with strong absorption across the full visible spectrum are desirable and rare in DSC reports. Comparing the effects within the proposed series, only a modest shift (10 nm) of the absorption maximum is observed based on the substitution position of the alkyne on ullazine with the position closest to the aryl group (4 position) giving the most red-shifted values. The ullazine-phenyl group substituent selection had little effect on the position of the absorption maximum.

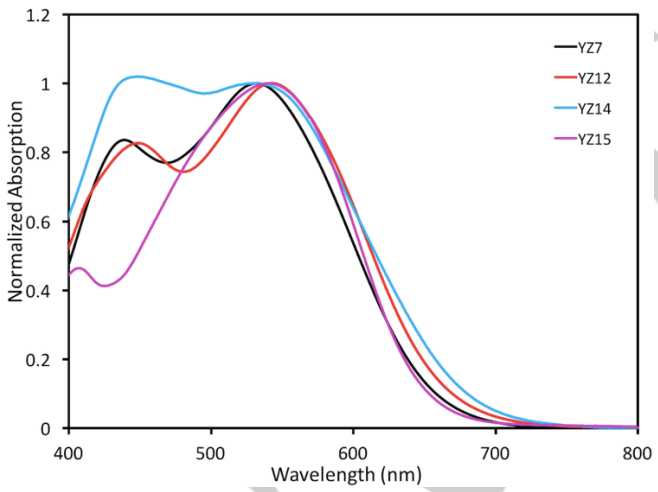

Figure 3. Absorption of **YZ7** (black line), **YZ12** (red line), **YZ14** (blue line), **YZ15** (purple line) measured in CH_2Cl_2.

Having established a desirable broad absorption spectrum for use in DSC devices, the dye energy levels were analyzed to evaluate the thermodynamic suitability of these dyes for DSCs. Cyclic voltammetry was used to measure the ground-state oxidation potentials ($E_{(S+/S)}$) (Table 1). The $E_{(S+/S)}$ values were measured within a range of 0.71-0.90 V versus NHE which are significantly more positive than the iodide/triiodide redox shuttle (0.35 V versus NHE). This indicates neutral dye regeneration is favorable with a driving force of 360-550 mV. The ground-state oxidation potential is similar or higher in energy for these dyes relative to a triphenylamine analogue (**C218**), which we attribute to the strong donation strength of the ullazine donor. The decrease in overpotential used to regenerate the dye is important to maximizing DSC device efficiencies, and maintaining high energy $E_{(S+/S)}$ values with NIR absorbing materials is critical for efficient solar-to-electric conversion at low energy with TiO_2 based DSC devices. The ullazine aryl substituents were found to have a significant effect on the dye ground state oxidation potential with the *para*-alkyoxyphenyl substituted dyes (**YZ7** and **YZ12**) having significantly lower energy $E_{(S+/S)}$ values relative to the di-*ortho*-alkyoxyphenyl substituted dyes (**YZ14** and **YZ15**). This highlights that the ullazine-phenyl group plays a key role in tunably tailoring $E_{(S+/S)}$ values. For favorable electron transfer to TiO_2 the dye excited-state oxidation potential ($E_{(S+/S^*)}$) should be higher in energy than -0.5 V versus NHE. The dye $E_{(S+/S^*)}$ values were calculated by subtracting the optical band gap (E_g^{opt}) found at the absorption onset from $E_{(S+/S)}$. $E_{(S+/S^*)}$ values for the dye series were found to be between -0.94 and -1.08 V versus NHE, which provides enough overpotential for injecting an electron from the photo-excited dye to the TiO_2 conduction band.

In addition to the suitable energetics found for each of the dyes, well positioned orbitals are required for efficient DSC devices. The dye lowest unoccupied molecular orbital (LUMO)

Table 1. Optical and electrochemical data for ullazine dyes **YZ7, YZ12, YZ14, YZ15**, **JD21**, and a TPA analogue **C218.**

dye	λ_{max} (nm)	ε ($M^{-1}cm^{-1}$)	$E_{(S+/S)}$ (V)	$E_{(S+/S^*)}$ (V)	E_g^{opt} (eV)
YZ7	532	29,000	0.90	-0.98	1.88
YZ12	543	28,000	0.90	-0.94	1.84
YZ14	537	28,000	0.71	-1.08	1.79
YZ15	549	26,000	0.84	-1.05	1.89
JD21	582	28,000	1.09	-0.94	2.03
C218	550	21,000	0.89	-1.06	1.95

*See experimental for detailed energy measurements and calculations.

should be positioned near the TiO_2 surface for efficient electron transfer from the dye to TiO_2. Additionally, the highest occupied molecular orbital (HOMO) should be positioned away from the TiO_2 surface to diminish back electron transfer from TiO_2 to the oxidized dye. Computational studies via density functional theory (DFT) were carried out to examine the position of the HOMO and LUMO at the B3LYP and 6-311G(d,p) level (**YZ7:** Figure 4, **YZ12**, **YZ14**, **YZ15**: Figure S2). The HOMO of the four ullazine-based dyes is primarily positioned on the ullazine motif with some delocalization onto the CPDT π-bridge. This position is ideal for good separation of the HOMO from the TiO_2 surface in space as the ullazine-donor is at the opposite end of the dyes relative to the anchor. The LUMO is partially delocalized over the CPDT bridge and primarily positioned on the acceptor/anchor. The position of both the HOMO and LUMO suggests these ullazine-based dyes can perform efficiently in DSC devices, and also suggests the ullazine-based D-π-A dyes are absorbing light via ICT.

Time-dependent DFT (TD-DFT) calculations were carried out to access the orbital contributions to each of the transitions observed in the absorption spectrum. For the ullazine D-π-A dyes, TD-DFT indicates the low energy transition band centered at ~530

10.1002/chem.201800030

nm is dominated by a HOMO to LUMO transition (99%) which confirm the ICT nature of these dyes (see Figure 4 for orbitals, see Table S1 for TD-DFT results). The high energy transition band at ~430 nm which led to a true panchromatic absorption in the UV-Vis-NIR absorption spectrum is attributed to a

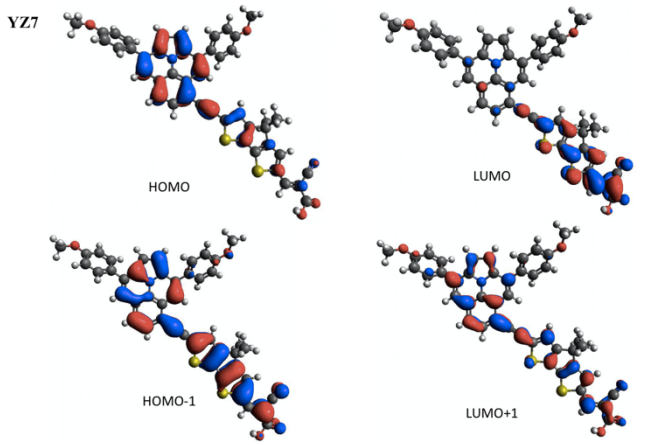

Figure 4. HOMO, LUMO, HOMO-1, LUMO+1 orbitals for dye **YZ7** given by DFT calculations at the B3LYP/6-311G(d,p) level.

combination of transitions from the HOMO-1 to LUMO (62%) and HOMO to LUMO+1 (36%). The HOMO-1 and LUMO+1 both have substantial involvement from the ullazine building block showing the importance of this building block in adding these strongly absorbing higher energy bands.

YZ7, **YZ12**, **YZ14** and **YZ15** were found to have a panchromatic solution absorption, properly positioned energy levels and properly positioned orbitals to perform well in DSC devices. Thus, devices were fabricated with the ullazine D-π-A dyes using TiO_2 as the semiconductor and iodine/triiodide as the redox shuttle (Figure 5 and Table 2). Sensitization of TiO_2 films is commonly done with EtOH:THF solutions for many organic dyes; however, the dyes examined in this report were not fully soluble at the desired 0.3 mM concentration. The addition of DMF to give a 4:1:2 (EtOH:THF:DMF) solution gave higher solubility and films were sensitized from this mixture. Initially the dyes were found to have PCE values of 2.1-4.4% with **YZ7** and **YZ15** having the highest performance according to the equation PCE = (J_{sc} x V_{oc} x FF)/I_0 where J_{sc} is the short circuit current density, V_{oc} is the open circuit voltage, *FF* is the fill factor, and I_0 is the sun intensity (Table 2, Figure 5). The dyes show similar *FF* values (0.68-0.70) and similar V_{oc} values (543-568 mV, except **YZ14** with 477 mV). The V_{oc} values were low in part due to significant LiI needing to be added to the cell electrolyte to increase J_{sc} values.

The largest change in dye performance was from the J_{sc} parameter, which ranged from 6.2-11.3 mA/cm^2. Such a broad variation in this parameter is somewhat surprising given the similarity of the dye orbital properties and dye energetics. Additionally, the two highest J_{sc} value dyes were **YZ7** and **YZ15,** which vary structurally the most in the series with a change at the position of the bridge-acceptor substitution and at the substituents on the aryl groups. To better understand this large variation in J_{sc} values, incident photon-to-current conversion efficiency (IPCE) measurements were undertaken. All of the dyes show a broad IPCE spectrum from 350 nm to approximately 800 nm, however the height of the IPCE spectrum varies dramatically with peak IPCE values in the following order **YZ14** (35%) < **YZ12** (55%) < **YZ15** (65%) = **YZ7** (65%). A slight increase in the high-energy region breadth explains the higher current from **YZ7** compared to **YZ15** observed from the IV curve measurements.

Table 2. DSC device parameters for **YZ7, YZ12, YZ14** and **YZ15**.

Dye	Voc/mV	Jsc/ mA cm^{-2}	FF	PCE (%)
YZ7	551	11.3	0.68	4.4
YZ12	543	9.6	0.70	3.8
YZ14	477	6.2	0.70	2.1
YZ15	568	10.9	0.69	4.4
YZ7*	559	14.1	0.67	5.6

See experimental for device details. *Indicates **YZ7** optimized device conditions.

The highest performing dye in the series (**YZ7**) was subjected to time correlated single photon counting (TCSPC) excited-state lifetime analysis to evaluate electron injection efficiency. **YZ7** shows excited-state lifetimes shorter than our instrument response time of (150 ps), both on TiO_2 and Al_2O_3 films, compared to 1.25 ns in DCM (Figure 6). This is surprising as a decreasing in excited-state lifetime on TiO_2 is commonly thought to correlate with electron injection; however, electron injection with in not possible Al_2O_3 as it is an insulator. Yet, Al_2O_3 shows a dramatic decrease in excited-state lifetime. A possible rationale

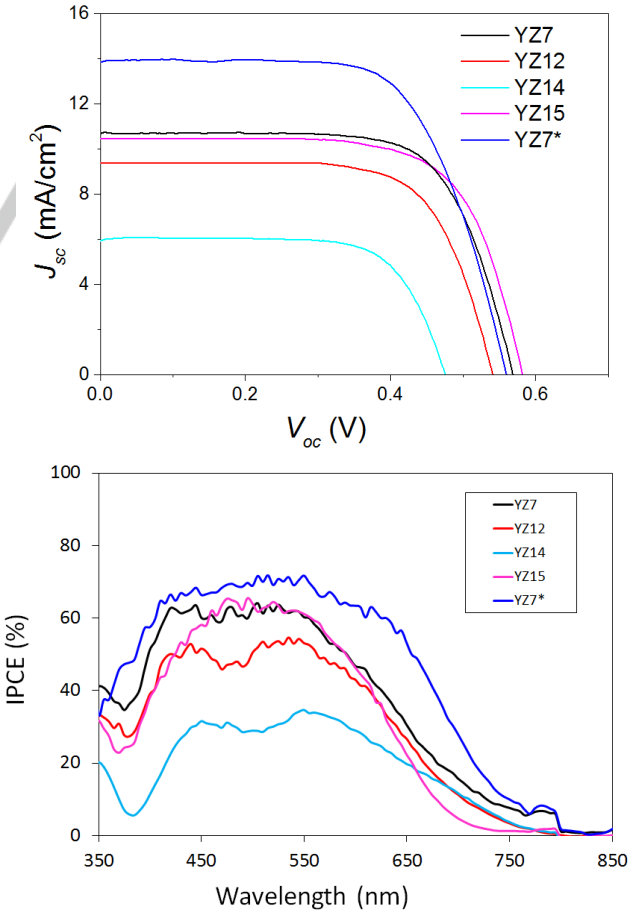

10.1002/chem.201800030

Figure 5. *J-V* curves (top) and IPCE (bottom) for DSC devices with **YZ7, YZ12, YZ14** and **YZ15.** *Indicates different dye sensitization solution was used (see Table 2 for details).

for this observation is heavy aggregation of the dye on film surfaces which diminishes excited-state lifetimes.

To evaluate this hypothesis, solid film UV-Vis absorption measurements were made for comparison to solution measurements for **YZ7** (Figure 7). Compared to solution measurements, the strength of the low energy and high energy transitions are reversed on the film. The results support our aggregation hypothesis as **YZ7** appears to aggregate heavily on solid films of TiO_2. CDCA is commonly used to disrupt aggregation and at very high loadings (100:1 CDCA:dye), the film absorption spectrum begins to look more like the solution spectrum in terms of relative transition intensity. Thus, the shorter excited state lifetime in the solid-state and the appearance of aggregation induced absorption may explain the need for higher LiI loading to achieve a higher injection free energy from the aggregates to TiO_2 by lowering TiO_2 conduction band (Table S4).

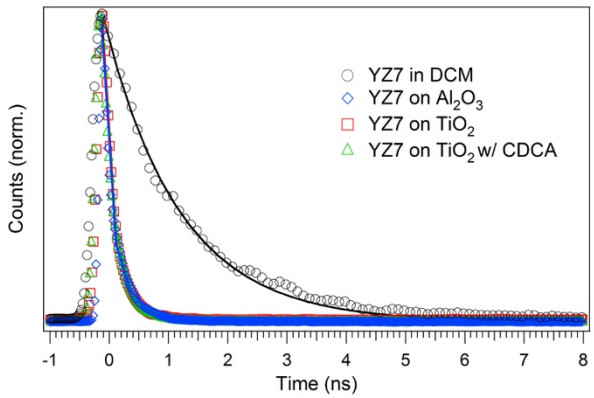

Figure 6: Time correlated single photon counting graph with **YZ7** in DCM solution, **YZ7** on Al_2O_3, **YZ7** on TiO_2 and **YZ7** on TiO_2 with CDCA.

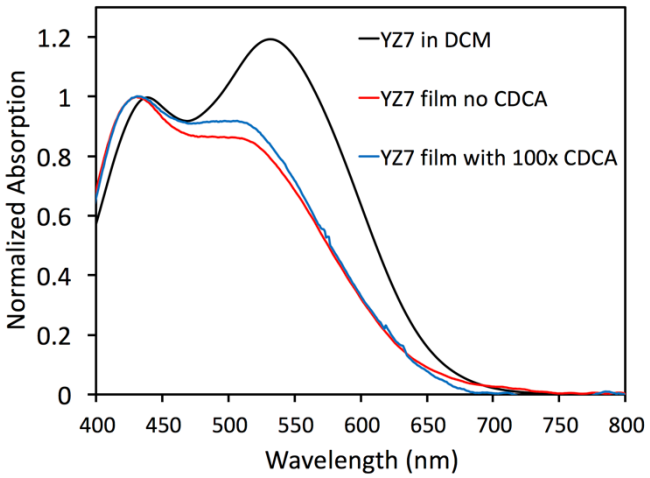

Figure 7: Normalized UV-Vis absorption of **YZ7** in DCM, and TiO_2 film absorption of **YZ7** with no CDCA and 100:1 CDCA:dye.

Given the similar energetics and absorption breadths, aggregation of these dyes on the TiO_2 surface is a potential PCE diminishing factor in this series. Evidence for this includes: (1) the IPCE spectrum onsets at a 100 nm longer wavelength than that of the DCM solution, (2) the absorption spectrum of the dye on TiO_2 shows the higher energy absorption band as the strongest transition while the solution absorption spectrum shows the lower energy absorption band as the strongest, (3) TCSPC studies show Al_2O_3 films decrease excited-state lifetimes dramatically compared to solution measurements, and (4) the addition of a co-sensitizer (**D35**) increased the IPCE intensity of **YZ7** in a region of the spectrum where **D35** does not absorb which implies disruption of aggregates (Figure S6). Attempts to diminish aggregation through addition of CDCA to the dye-deposition solution only shows a modest change in the dye-TiO_2 film absorption spectrum and no significant enhancement of device performance. To evaluate the effects of deposition solvent with the best performing dye, **YZ7**, a series of solvents were examined (Table S2, Figure S4). The PCE efficiency varies substantially with deposition solvent from 3.4-5.6% PCE. The best conditions were found to be deposition of **YZ7** from acetonitrile:*tert*-butanol:chlorobenzene (1:1:1.2,v/v/v) with 10:1 CDCA:dye. The IPCE curve of **YZ7** under optimized conditions shows an increase in percent intensity from 350 nm to 800 nm with a peak value of 75%. The integrated current under the IPCE curve is in good agreement with the short-circuit current density (J_{sc}) of 14.1 mA/cm^2 measured under AM 1.5 conditions. The measured J_{sc} combined with an open-circuit voltage (V_{oc}) of 559 mV and fill factor (FF) of 0.67 gives the highest power conversion efficiency (PCE) of the series at 5.6%. These results show that the Ullazine donor is exceptional at the introduction of desirable dye properties (panchromatic light absorption, multiple transitions in the UV-Vis spectrum, and maintaining high energy oxidation potentials); however, in the solid state the aggregation of these dyes leads to diminished device performances which must be carefully optimized to increase IPCE response and device PCE.

Conclusions

In summary, we have designed and synthesized a series of metal-free ullazine based D-π-A dyes for the first time. These dyes were characterized by UV-Vis-NIR absorption spectroscopy, cyclic voltammetry, and computational analysis, which reveal suitable characteristics for use in DSC devices. The broad, near uniform solution absorption intensity from 350-700 nm is particularly desirable for DSC applications. This dramatic change in absorption spectrum from the prior reports on D-A ullazine sensitizers with relatively narrow absorption spectrum response is encouraging. A PCE of 5.6% was obtained for the highest performing dye in the series (**YZ7**) with an IPCE onset of 800 nm. Given the relatively few metal-free dyes reaching 800 nm in an IPCE spectrum this dye-design warrants further investigation. TCSPC studies and film absorption measurements show substantial aggregation of the dyes on the TiO_2 surface. This strongly suggests the diminishment in IPCE peak value (75% with a maximum of 90%) is the result of surface aggregation. Future

dye designs will focus added substituents to the ullazine building block which are known to dramatically reduce dye aggregation.

Experimental Section

General Information. All commercially obtained reagents were used as received. 3,9-bis(4-(hexyloxy)phenyl) indolizino[6,5,4,3-ija]quinoline-5-carbaldehyde (**6a**) and 3,9-bis(4-(hexyloxy)phenyl)indolizino[6,5,4,3-ija]quinoline-4-carbaldehyde (**7a**) were made according to literature.[3c] 6-bromo-4,4-dihexyl-4H-cyclopenta[2,1-b:3,4-b']dithiophene-2-carbaldehyde (**10**) was prepared according to literature procedure.[11] 1-(2,6-dibromophenyl)-1H-pyrrole (**3**) was prepared according to literature procedure.[3c] Thin-layer chromatography (TLC) was conducted with Sorbtech silica XHL TLC plates and visualized with UV. Flash column chromatography was performed with Silicycle ultrapure silica gel P60, 40-63 μm (230-400 mesh). Reverse phase column chromatography was performed with premium grade C18 silica gel from Sorbent technologies. ^{1}H NMR spectra were recorded on Bruker Avance-300 (300 MHz) and Bruker Avance DRX-500 (500 MHz) spectrometers and are reported in ppm using solvent as an internal standard ($CDCl_3$ at 7.28 ppm). NMR data is reported as s = singlet, d = doublet, t = triplet, q = quartet, p = pentet, m = multiplet, br = broad, ap = apparent, dd = doublet of doublets, and coupling constant(s) are in Hertz, followed by integration information. UV−Vis-NIR spectra were measured with a Cary 5000 instrument. HPLC measurements were taken using an Agilent 1100A HPLC instrument, equipped with an Agilent Eclipse Plus C18 column and UV-Vis detector. 90% isopropanol: 10% water was used as the mobile phase at 0.3 ml/min for all the measurement. HRMS spectra were obtained with a QTOF HRMS utilizing nanospray ionization. The mass analyzer was set to the 400−2000 Da range. CV data was collected with a CH Instruments CHI600E instrument.

Electrochemical Characterization. Cyclic voltammetry was measured with a 0.1 M Bu_4NPF_6 in CH_2Cl_2 solution using a glassy carbon working electrode, platinum reference electrode, and platinum counter electrode with ferrocene as an internal standard. Values are reported versus NHE with ferrocene taken as 0.70 V vs NHE. $E_{(S+/S^*)}$ is calculated from the equation $E_{(S+/S^*)} = E_{(S+/S)} - E_g^{opt}$. E_g^{opt} is estimated from the onset of the absorption spectrum and converted from nanometers to eV with the equation: $E_g^{opt} = 1240/\lambda_{onset.}$

Computational Protocol. MM2 energy minimization in ChemBio3D Ultra (version:13.0.2.3021) was used for the initial energy minimization of the four dyes. Dihedral angles for the relevant groups were set to values between the global minimum and the next local minimum on the conformation energy diagram as calculated by ChemBio3D. Accurate geometry optimizations were performed sequentially by density functional theory (DFT) using Guassian09 with the B3LYP functional with the following basis sets: first 3-21g, second 6-31g (d,p) and finally 6-311g (d,p). No imaginary frequencies were observed for the optimized geometries. Time-dependent density functional theory (TD-DFT) computations were performed with optimized geometries and with the B3LYP functional and 6-311g (d.p) basis set to compute the lowest energy 10 vertical transitions and oscillator strengths. Orbital images were prepared with Avogadro 1.0.3 with an iso value of 0.30.

Time Correlated Single Photon Counting (TCSPC) Measurements: Fluorescence lifetime curves were obtained using the 485 nm line of an LDH series 485B pulsed diode laser (pulse width approx. 100 ps) as the excitation source and emission was detected using a PicoQuant PDM series single photon avalanche diode (time resolution approx. 50 ps) and TimeHarp 260 time correlated single photon counter (25 ps resolution). The alumina paste was prepared by following the reported procedure with the following modifications.[12] 167 mg of Al_2O_3 NPs (particle size ~ 150 mesh, pore size = 58 Å, surface area = 155 m^2/g, SigmaAldrich) was dispersed in a 5 mL solution containing α-terpineol/ethylcellulose (Sigma aldrich # 46080, 48.0-49.5% (w/w) ethoxyl basis) (ethylcellulose content: 6 wt % of *α*-terpineol, 280 mg) with 5 ml of acetone. The suspension was kept under stirring conditions over a period of 2 days, after which the remaining acetone was removed by rotary evaporator. The α-terpineol/ethylcellulose mixture was first prepared by completely dissolving ethylcellulose in α-terpineol in the presence of 5 ml ethanol, once dissolved excess ethanol was removed by rotary evaporator. The prepared paste was then used to screen print films with a Sefar screen (54/137–64W) resulting in 1 μm thick films on TEC 15 FTO glass. Before its use, the TEC 15 was cleaned by submerging in a 0.2% Deconex 21 aqueous solution and sonicated for 15 minutes at room temperature. The FTO glass was rinsed with water and sonicated in acetone 10 minutes followed by sonication in ethanol for 10 minutes. Finally, after paste printing and drying on a hot plate for 7 minutes at 125°C, substrates were then sintered with progressive heating from 125°C (5 minute ramp from r.t., 5 minute hold) to 325°C (15 minute ramp from 125oC, 5 minute hold) to 375°C (5 minute ramp from 325°C, 5 minute hold) to 450°C (5 minute ramp from 375°C, 15 minute hold) to 500°C (5 minute ramp from 450°C, 15 minute hold) using a programmable furnace (Vulcan® 3-Series Model 3-550). After cooling to room temperature, the electrodes were dipped in the 0.3 mM dye solution for 16 hours and used as it is for TCSPC measurements.

Photovoltaic Measurements: Current-Voltage curve photovoltaic characteristics were measured using a 150 W Xenon lamp (Model SF150B, SCIENCETECH Inc. Class ABA) solar simulator equipped with an AM 1.5 G filter for a less than 2% spectral mismatch. Prior to each measurement, the solar simulator output was calibrated with a KG5 filtered mono-crystalline silicon NREL calibrated reference cell from ABET Technologies (Model 15150-KG5). The current density-voltage characteristics of each cell was obtained with a Keithley digital source-meter (Model 2400). The incident photon-to-current conversion efficiency was measured with an IPCE instrument manufactured by Dyenamo comprised of a 175 W Xenon lamp (CERMAX, Model LX175F), monochromator (Spectral Products, Model CM110, Czerny-Turner, dual-grating), filter wheel (Spectral Products, Model AB301T, fitted with filter AB3044 [440 nm high pass] and filter AB3051 [510 nm high pass]), a calibrated UV-enhanced silicon photodiode reference, and Dyenamo issued software.

Device Fabrication: For the photoanode, TEC 10 glass was purchased from Hartford Glass. Once cut into 2x2 cm squares, the substrate was submerged in a 0.2% Deconex 21 aqueous solution and sonicated for 15 minutes at room temperature. The electrodes were rinsed with water and sonicated in acetone 10 minutes followed by sonication in ethanol for 10 minutes. Finally, the electrodes were placed under UV/ozone for 15 minutes (UV-Ozone Cleaning System, Model ProCleaner by UVFAB Systems). A compact TiO_2 underlayer is then applied by pretreatment of the substrate submerged in a 40 mM $TiCl_4$ solution in water (prepared from 99.9% $TiCl_4$ between 0-5°C). The submerged substrates (conductive side up) were heated for 30 minutes at 70°C. After heating, the substrates were rinsed first with water then with ethanol. The photoanode consists of thin TiO_2 electrodes comprised of a 10 μm mesoporous TiO_2 layer (particle size, 20 nm, Dyesol, DSL 18NR-T) for **YZ7**-**YZ15** for devices using the iodine redox shuttle and a 5.0 μm TiO_2 scattering layer (particle size, 100 nm, Solaronix R/SP). Both layers were printed from a Sefar screen (54/137–64W). Between each print, the substrate was heated for 7 minutes at 125°C and the thickness was measured with a profilometer (Alpha-Step D-500 KLA Tencor). The substrate was then sintered with progressive heating from 125°C (5 minute ramp from r.t., 5 minute hold) to 325°C (15 minute ramp from 125°C, 5 minute hold) to 375°C (5 minute ramp from 325°C, 5 minute hold) to 450°C (5 minute ramp from 375°C, 15 minute hold) to 500°C (5 minute ramp from 450°C, 15 minute hold) using a programmable furnace (Vulcan® 3-Series Model 3-550). The cooled sintered photoanode was soaked 30 min at 70°C in a 40 mM $TiCl_4$ water solution and heated again at 500°C for 30 minutes prior to sensitization. The complete working electrode was prepared by

immersing the TiO_2 film into the dye solution overnight at room temperature. The solution is 0.3 mM of dye in different solvent mixtures (Table S2). For preparing counter electrodes, 2x2 cm squares TEC 7 FTO glass was drilled using a Dremel-4000 with Dremel 7134 Diamond Taper Point Bit with FTO side protected by tape. Electrodes were washed with water followed by a 0.1M HCl in EtOH wash and sonication in acetone bath for 10 minutes. These washed FTO electrodes were then dried at 400°C for 15 minutes. A thin layer of Pt-paste (Solaronix, Platisol T/SP) was slot printed on the FTO, and the printed electrodes were then heated at 450°C for 10 minutes. After allowing them to cool to room temperature, the working electrodes were then sealed to the Pt-FTO electrodes with a 25 µm thick hot melt film (Solaronix, "Meltonix", Surlyn) by heating the system at 130°C under 0.2 psi pressure for 1 minute. Devices were completed by filling the electrolyte through the pre-drilled holes in the counter electrodes, and finally the holes were sealed with a Surlyn circle and a thin glass cover by heating at 130°C under a pressure of 0.1 psi for 25 seconds. Finally, soldered contacts were added with a MBR Ultrasonic soldering machine (model USS-9210) with a solder alloy (Cerasolzer wire diameter 1.6 mm, item # CS186-150). A circular black mask (active area 0.15 cm^2) was punched from black tape and used in the subsequent photovoltaic studies. Film absorption was done using TEC 15 glass with 3 µm mesoporous TiO_2 film (particle size, 20 nm, Dyesol, DSL 18NR-T), and progressively heated as described previously.

Synthetic Data

2-ethynyl-1,3-bis(hexyloxy)benzene (2b): To a flame dried flask was added freshly prepared dibromomethyl-triphenylphosphonium bromide[3] (38.6 g, 75.3 mmol, 2.02 equiv.) and tetrahydrofuran (377 ml). In one portion, potassium *tert*-butoxide (7.93 g, 70.8 mmol, 1.90 equiv.) was added and the mixture stirred at ambient temperature for 3 minutes. A solution of **1b**[1] (11.4 g, 37.3 mmol, 1.0 equiv.) in tetrahydrofuran (63.2 ml) was added to the reaction mixture via cannula, and the resulting mixture was stirred at room temperature for 10 minutes. The reaction was cooled to -78°C and potassium *tert*-butoxide (20.8 g, 187 mmol, 5.0 equiv.) was added in one portion following gradual warming to ambient temperature. After 1.5 hours, the reaction mixture was diluted with dichloromethane and rinsed with water, dried by Na_2SO_4 and evaporated. The crude mixture was purified through silica gel chromatography using 20% dichloromethane: hexane was the eluent to get clear oil. (8.51 g, 75%). ^{1}H NMR (500 MHz, $CDCl_3$) δ = 7.18 (t, *J* = 8.4 Hz, 1H), 6.50 (d, *J* = 8.5 Hz, 2H), 4.03 (t, *J* = 6.7 Hz, 4H), 3.48 (s, 1H), 1.95-1.70 (m, 4H), 1.60-.142 (m, 4H), 1.42-1.22 (m, 8H), 0.95-0.92 (ap t, 6H). ^{13}C NMR (125 MHz, $CDCl_3$) δ = 161.8, 129.9, 104.5, 101.4, 85.1, 76.3, 68.9, 31.6, 29.1, 25.6, 22.6, 14.0. IR (neat, cm^{-1}): 3324, 2936, 2918, 2852, 1583, 1453, 1391, 1289, 1251, 1092, 894, 771. HRMS (ESI) *m/z* calc'd (positive mode) for $C_{20}H_{31}O_2$ $[M+H]^+$ 303.2324, found 303.2304.

1-(2,6-bis((2,6-bis(hexyloxy)phenyl)ethynyl)phenyl)-1H-pyrrole (4b): To a flame dried N_2 filled flask was added 1-(2,6-dibromophenyl)-1H-pyrrole (**3**),[3c] (3.53 g, 11.3 mmol, 1.0 equiv.), 2-ethynyl-1,3-bis(hexyloxy)benzene (**2b**) (8.51 g, 28.2 mmol, 2.4 equiv.), CuI (89.4 mg, 0.47 mmol, 0.04 equiv.), $Pd[P(tBu)_3]_2$ (359 mg, 0.70 mmol, 0.06 equiv.), dioxane (23.5 ml), and diisopropylamine (4.21 ml, 28.1 mmol, 2.4 equiv.). The mixture was stirred at room temperature overnight. The reaction mixture was then extracted with DCM and H_2O. The crude mixture was purified through silica gel chromatography using 5% ether: hexane as the eluent to give the pure product (7.22 g, 83%). ^{1}H NMR (500 MHz, $CDCl_3$) δ = 7.65 (d, *J* =7.7 Hz, 2H), 7.36 (br s, 2H), 7.27 (t, *J* = 7.7 Hz, 1H), 7.18 (t, *J* = 8.3 Hz, 2H), 6.51 (d, *J* = 8.3 Hz, 4H), 6.28 (br s, 2H), 4.02 (t, *J* = 6.4 Hz, 8H), 1.95-1.80 (m, 8H), 1.63-1.33 (m, 24H), 0.95-0.90 (ap t, 12H). ^{13}C NMR (125 MHz, $CDCl_3$) δ = 161.3, 141.4, 133.7, 129.9, 126.0, 122.8, 121.7, 108.2, 104.6, 102.4, 94.3, 87.5, 69.0, 31.8, 29.3, 25.9, 22.8, 14.2. IR (neat, cm^{-1}): 3098, 3057, 2925, 2860, 1578, 1454, 1383, 1297, 1251, 1093, 1012, 901. HRMS (ESI) *m/z* calc'd (positive mode) for $C_{50}H_{66}O_4N$ $[M+H]^+$ 744.4992, found 744.5026.

3,9-bis(2,6-bis(hexyloxy)phenyl)-4,4a1-dihydroindolizino[6,5,4,3-*ija*]quinolone (5b): To a flame dried, N_2 filled flask was added 1-(2,6-bis((2,6-bis(hexyloxy)phenyl)ethynyl)phenyl)-1H-pyrrole (**4b**), (6.90 mg, 9.27 mmol, 1.0 equiv.), $InCl_3$ (1.23 g, 5.58 mmol, 0.60 equiv.) and toluene (46.5 ml, 0.2 M). The mixture was stirred at 100°C overnight. The reaction mixture was filtered through a pad of silica gel with 5% ethylacetate: hexane as eluent to give the crude product after evaporation. Then, the mixture was purified through silica gel chromatography with 10% dichloromethane:hexanes to give the final pure product (1.99 g, 29%). ^{1}H NMR (500 MHz, $CDCl_3$) δ = 7.51-7.42 (m, 3H), 7.37 (t, *J* = 8.4 Hz, 2H), 7.20 (s, 2H), 6.76 (d, *J* =8.4 Hz, 4H), 6.60 (s, 2H), 4.10-3.88 (m, 8H), 1.70-1.49 (m, 8H), 1.32-1.05 (m, 24H), 0.79 (t, *J* = 6.7 Hz, 12H). ^{13}C NMR (75 MHz, $CDCl_3$) δ = 158.3, 132.9, 129.1, 127.0, 126.4, 126.1, 123.0, 121.0, 118.3, 117.2, 105.7, 105.2, 69.0, 31.4, 29.0, 25.6, 22.5, 13.9. IR (neat, cm^{-1}): 3585, 3174, 3055, 2920, 2855, 2334, 1585, 1452, 1410, 1365, 1244, 1091, 1030, 863. HRMS (ESI) *m/z* calc'd (positive mode) for $C_{50}H_{65}O_4NCs$ $[M+Cs]^+$ 876.3968, found 876.3904.

3,9-bis(2,6-bis(hexyloxy)phenyl)indolizino[6,5,4,3-*ija*]quinoline-5-carbaldehyde (6b): To a flame dried, N_2 filled round bottom flask was added 3,9-bis(2,6-bis(hexyloxy)phenyl)-4,4a1-dihydroindolizino[6,5,4,3-*ija*]quinolone (**5b**) (1.90 g, 2.6 mmol, 1.0 equiv.), dichloroethane (8.4 ml, 0.13 M), and anhydrous *N,N*-dimethylformamide (0.48 ml, 6.24 mmol, 2.4 equiv.). The mixture was stirred at room temperature while $POCl_3$ (0.60 ml, 6.24 mmol, 2.4 equiv.) was added dropwise via syringe. The reaction was stirred for 5 hours at room temperature to give a red solution. The reaction mixture was then diluted with a 50 mL ~1:1 mixture of dichloromethane:NaOAc (sat. aq.) for 2 hours. The product was purified with silica chromatography using 10% dichloromethane:hexanes to give an orange oil (156 mg, 7.8 %) as the major side product. ^{1}H NMR (500 MHz, $CDCl_3$) δ = 10.32 (s, 1H), 8.95 (s, 1H), 7.89 (d, *J* =8.2 Hz, 1H), 7.53 (d, *J* =8.2 Hz, 1H), 7.44 (s, 1H), 7.41-7.32 (m, 2H), 6.91-6.96 (m, 2H), 6.73 (dd, *J* =2.9 Hz, *J* =2.9 Hz, 4H), 4.01-3.82 (m, 8H), 1.55-1.42 (m, 8H), 1.22-0.98 (m, 24H), 0.77-0.59 (m, 12H). ^{13}C NMR (75 MHz, $CDCl_3$) δ = 191.0, 158.1, 158.0, 131.9, 131.2, 130.8, 129.8, 129.6, 129.5, 128.4, 127.9, 126.6, 121.7, 121.2, 119.2, 116.7, 116.5, 115.9, 109.1, 108.7, 105.4, 105.3, 68.9, 68.8, 31.3, 31.3, 28.9, 28.9, 25.5, 25.5, 22.4, 22.4, 13.8, 13.8. IR (neat, cm^{-1}): 3489, 3284, 3186, 3111, 2922, 2855, 2714, 2337, 1664, 1582, 1453, 1350, 1297, 1245, 1185, 1092, 1028, 940. HRMS (ESI) *m/z* calc'd (positive mode) for $C_{51}H_{65}O_5NCs$ $[M+Cs]^+$ 904.3917, found 904.3705.

3,9-bis(2,6-bis(hexyloxy)phenyl)indolizino[6,5,4,3-*ija*]quinoline-4-carbaldehyde (7b): This material was formed as the major product during the formylation reaction to form 3,9-bis(2,6-bis(hexyloxy)phenyl)indolizino[6,5,4,3-*ija*]quinoline-5-carbaldehyde (**6b**). 3,9-bis(2,6-bis(hexyloxy)phenyl)indolizino[6,5,4,3-*ija*]quinoline-4-carbaldehyde (**7b**) was observed as a slightly lower R_f than 3,9-bis(2,6-bis(hexyloxy)phenyl)indolizino[6,5,4,3-*ija*]quinoline-5-carbaldehyde (**6b**) on TLC with 10% dichloromethane:hexane as eluent. The product was isolated by silica chromatography with 10% dichloromethane:hexanes to give a yellow solid (1.09 g, 55%). ^{1}H NMR (500 MHz, $CDCl_3$) δ = 9.44 (s, 1H), 7.59-7.50 (m, 3H), 7.46 (s, 1H), 7.64-7.49 (m, 2H), 7.23 (s, 1H), 7.08 (s, 1H), 6.71 (dd, *J* = 2.7 Hz, 2.7 Hz, 4H), 4.29-3.78 (m, 8H), 1.89-1.41 (m, 8H), 1.41-0.98 (m, 24H), 0.72 (ap t, 12H). ^{13}C NMR (125 MHz, $CDCl_3$) δ = 186.6, 158.1, 157.8, 131.9, 130.4, 130.3, 129.7, 128.2, 127.4, 126.7, 126.4, 125.8, 125.2, 124.4, 123.7, 120.9, 120.4, 120.4, 116.4, 115.4, 105.3, 105.3, 105.3, 104.7, 68.7, 68.7, 31.3, 31.2, 29.0, 28.9, 25.6, 25.5, 22.4, 22.4, 13.8, 13.8. IR (neat, cm^{-1}): 3311, 3180, 3057, 2924, 2858, 2335, 1648, 1587, 1523, 1454, 1386, 1290, 1245, 1194, 1093, 908, 879. HRMS (ESI) *m/z* calc'd (positive mode) for $C_{51}H_{65}O_5NCs$ $[M+Cs]^+$ 904.3917, found 904.3762.

5-ethynyl-3,9-bis(4-(hexyloxy)phenyl)indolizino[6,5,4,3-*ija*]quinoline (8a): To a flame dried flask was added freshly prepared dibromomethyl-triphenylphosphonium bromide[13] (2.01g, 4.04 mmol, 2.02 equiv.) and tetrahydrofuran (20.2 ml). In one portion, potassium *tert*-butoxide (426 mg, 3.80 mmol, 1.90 equiv.) was added and the mixture stirred at ambient temperature for 3 minutes. A solution of 3,9-bis(4-(hexyloxy)phenyl)indolizino[6,5,4,3-*ija*]quinoline-5-carbaldehyde (**6a**)[3c] (1.149 g, 2.0 mmol, 1.0 equiv.) in tetrahydrofuran (3.4 ml) was added to the reaction mixture via cannula, and the resulting mixture was stirred at room temperature for 10 minutes. The reaction was cooled to negative 78°C and potassium *tert*-butoxide (426 mg, 3.80 mmol, 5.0 equiv.) was added in one portion following gradual warming to ambient temperature. After 1.5 hours, the reaction mixture was diluted with dichloromethane and rinsed with water, dried by Na_2SO_4 and evaporated. The crude product was filtered through a pad of silica gel, eluting with 50 % dichloromethane/hexanes to give the desired product as a yellow oil (1.08 g, 95%). ^{1}H NMR (500 MHz, $CDCl_3$) δ = 7.80 (d, *J* = 8.6 Hz, 2H), 7.75 (d, *J* = 8.6 Hz, 2H), 7.69 (s, 1H), 7.65 (d, *J* = 8.1 Hz, 1H), 7.44 (d, *J* = 8.1 Hz,

1H), 7.21 (s, 1H), 7.10 (d, *J* = 7.3 Hz, 2H), 7.08 (d, *J* = 7.3 Hz, 2H). 4.21-3.95 (m, 4H), 3.53 (s, 1H), 2.00-1.75 (m, 4H), 1.74-1.20 (m, 12H), 0.96 (t, *J* = 6.8 Hz, 6H). ^{13}C NMR (125 MHz, $CDCl_3$) δ = 159.5, 159.5, 133.9, 133.6, 131.4, 130.8, 130.6, 129.6, 129.6, 129.4, 128.2, 128.1, 127.5, 127.1, 127.0, 126.3, 118.5, 118.2, 117.3, 114.7, 114.7, 109.8, 107.2, 82.8, 81.7, 68.2, 31.7, 29.8, 29.4, 28.3, 25.9, 22.7, 14.2 IR (neat, cm^{-1}): 3312, 2925, 2855, 2334, 2093, 1602, 1503, 1493, 1389, 1299, 1276, 1240, 1171, 1110, 1032, 824, 792. HRMS (ESI) *m/z* calc'd (positive mode) for $C_{40}H_{41}O_2NCs$ $[M+Cs]^+$ 700.2192, found 700.2186.

3,9-bis(2,6-bis(hexyloxy)phenyl)-5-ethynylindolizino[6,5,4,3-*ija*]quinoline (8b): The synthesis follows the same procedure as 5-ethynyl-3,9-bis(4-(hexyloxy)phenyl)indolizino[6,5,4,3-*ija*]quinoline (**8a**) except 3,9-bis(2,6-bis(hexyloxy)phenyl)indolizino[6,5,4,3-*ija*]quinoline-5-carbaldehyde (**6b**, 64.3 mg) was used in place of 3,9-bis(4-(hexyloxy)phenyl)indolizino[6,5,4,3-*ija*]quinoline-5-carbaldehyde (**6a**). The reaction mixture was extracted by DCM and H_2O, dried with Na_2SO_4 and evaporated. The crude mixture was purified through silica gel chromatography using 50% dichloromethane:hexane as the eluent to give a pure yellow oil (54.3 mg, 85%). ^{1}H NMR (500 MHz, $CDCl_3$) δ = 7.67 (s, 1H), 7.63 (d, *J* = 8.0 Hz, 1H), 7.43-7.31 (m, 3H), 7.23 (s, 1H), 6.68-6.60 (m, 6H), 4.20-3.80 (m, 8H), 3.43 (s, 1H), 1.70-1.42 (m, 8H), 1.29-1.00 (m, 24H), 0.73 (ap t, 12H). ^{13}C NMR (75 MHz, $CDCl_3$) δ = 158.2, 158.2, 132.1, 129.3, 129.2, 127.8, 127.5, 127.4, 127.3, 127.2, 126.5, 120.9, 119.9, 117.5, 116.9, 116.7, 109.0, 106.5, 106.4, 105.5, 105.5, 105.5, 83.3, 80.6, 68.9, 68.9, 31.3, 31.3, 28.9, 28.9, 25.5, 25.5, 22.4, 22.4, 13.8, 13.8. IR (neat, cm^{-1}): 3307, 2927, 2862, 1591, 1457, 1421, 1395, 1366, 1297, 1247, 1098, 1027, 872. HRMS (ESI) *m/z* calc'd (positive mode) for $C_{51}H_{65}O_5NCs$ $[M+Cs]^+$ 900.3968, found 900.3716.

4-ethynyl-3,9-bis(4-(hexyloxy)phenyl)indolizino[6,5,4,3-*ija*]quinoline (9a): The synthesis follows the same procedure as 5-ethynyl-3,9-bis(4-(hexyloxy)phenyl)indolizino[6,5,4,3-*ija*]quinoline (**8a**) except 3,9-bis(4-(hexyloxy)phenyl)indolizino[6,5,4,3-*ija*]quinoline-4-carbaldehyde (**7a**, 280 mg)[3c] was used in place of 3,9-bis(4-(hexyloxy)phenyl)indolizino[6,5,4,3-*ija*]quinoline-5-carbaldehyde (**6a**). The crude mixture was purified through silica gel chromatography using 50% dichloromethane:hexanes as the eluent to give the pure product (253 mg, 91%). ^{1}H NMR (300 MHz, Acetone-d_6) δ = 7.87 (d, *J* = 6.7 Hz, 1H), 7.70 (d, *J* = 8.5 Hz, 2H) , 7.67 (d, *J* = 8.4 Hz, 2H), 7.60 (d, *J* = 7.7 Hz, 1H), 7.52 (t, *J* = 7.7 Hz, 1H), 7.34 (s, 1H), 7.13-6.97 (m, 5H), 6.84 (d, *J* = 4.3 Hz, 1H), 4.13-4.00 (m, 4H), 3.99 (s, 1H), 1.90-1.71(m, 4H), 1.60-1.25 (m, 12H), 1.11-0.80 (m, 6H). ^{13}C NMR (75 MHz, acetone-d_6) δ = 159.6, 137.3, 132.6, 131.2, 130.9, 130.2, 129.2, 128.6, 127.5, 126.9, 125.7, 125.0, 124.1, 120.2, 119.3, 118.6, 114.7, 114.0, 109.1, 108.6, 107.0, 86.4, 80.2, 67.8, 67.8, 31.5, 25.6, 25.6, 22.4, 13.5. IR (neat, cm^{-1}): 3279, 2924, 2856, 1976, 1604, 1507, 1428, 1406, 1395, 1360, 1278, 1244, 1174, 1116, 1071, 1027, 830. HRMS (ESI) *m/z* calc'd (positive mode) for $C_{40}H_{41}O_2NCs$ $[M + Cs]^+$ 700.2192, found 700.2178.

3,9-bis(2,6-bis(hexyloxy)phenyl)-4-ethynylindolizino[6,5,4,3-*ija*]quinoline (9b): The synthesis follows the same procedure as 5-ethynyl-3,9-bis(4-(hexyloxy)phenyl)indolizino[6,5,4,3-*ija*]quinoline (**8a**) except 3,9-bis(2,6-bis(hexyloxy)phenyl)indolizino[6,5,4,3-*ija*]quinoline-4-carbaldehyde (**7b**, 466 mg) was used in place of 3,9-bis(4-(hexyloxy)phenyl)indolizino[6,5,4,3-*ija*]quinoline-5-carbaldehyde (**6a**). The reaction mixture was extracted by dichloromethane and H_2O, dried with Na_2SO_4 and evaporated. The crude mixture was purified through silica gel chromatography using 50% dichloromethane:hexanes as the eluent to give a yellow oil (153 mg, 33%). ^{1}H NMR (300 MHz, $CDCl_3$) δ = 7.44 (br s, 3H), 7.38-7.25 (m, 2H), 7.18 (d, *J* = 8.5 Hz, 2H), 6.70 (d, *J* = 8.3 Hz, 2H), 6.64 (ap d, 3H), 4.08-3.80 (m, 8H), 2.59 (s, 1H), 1.68-1.40 (m, 8H), 1.38-0.99 (m, 24H), 0.81-0.59 (m, 12H). ^{13}C NMR (125 MHz, $CDCl_3$) δ = 158.8, 158.1, 132.4, 129.3, 129.2, 128.4, 126.6, 126.1, 126.0, 126.0, 125.9, 123.6, 123.0, 122.3, 119.3, 119.1, 116.3, 116.2, 109.7, 105.4, 105.0, 99.2, 79.2, 77.6, 68.9, 68.9, 31.3, 31.3, 29.0, 28.9, 25.6, 25.5, 22.4, 22.4, 13.8, 13.8. IR (neat, cm^{-1}): 3310, 2926, 2861, 1589, 1457, 1388, 1296, 1247, 1097, 871. HRMS (ESI) *m/z* calc'd for (positive mode) $C_{52}H_{66}O_4N$ $[M+H]^+$ 768.4992, found 768.4495.

6-((3,9-bis(4-(hexyloxy)phenyl)indolizino[6,5,4,3-*ija*]quinolin-5-yl)ethynyl)-4,4-dihexyl-4H-cyclopenta[2,1-*b*:3,4-*b'*]dithiophene-2-carbaldehyde (11a): To a flame dried N_2 filled round bottom flask was added CuI (0.67 mg, 0.003 mmol, 0.04 equiv.), dioxane (0.18 ml), diisopropylamine (0.03 ml, 0.211 mmol, 2.4 equiv.), $Pd[P(t\text{-}Bu)_3]_2$ (2.69 mg, 0.005 mmol, 0.06 equiv.), 5-ethynyl-3,9-bis(4-(hexyloxy)phenyl)indolizino[6,5,4,3-*ija*]quinoline (**8a**) (60 mg, 0.106 mmol, 1.2 equiv.), and 6-bromo-4,4-dihexyl-4H-cyclopenta[2,1-b:3,4-b']dithiophene-2-carbaldehyde (**10**)[11] (40.0 mg, 0.088 mmol, 1.0 equiv.). The mixture was stirred at room temperature overnight. The reaction mixture was then diluted with dichloromethane and extracted with dichloromethane/H_2O, dried by Na_2SO_4 and evaporated. The product was then purified through silica gel chromatography with 50% diethyl ether:hexanes to give the desired product as a red solid (79 mg, 97%). ^{1}H NMR (300 MHz, $CDCl_3$) δ = 9.88 (s, 1H), 7.82 (d, *J* = 8.5 Hz, 2H), 7.76 (d, *J* = 8.6 Hz, 2H), 7.70 (s, 1H), 7.66 (d, *J* = 8.1 Hz, 1H), 7.59 (s, 1H), 7.46 (d, *J* = 8.0 Hz, 1H), 7.29 (d, *J* = 5.7 Hz, 1H), 7.22 (br. s, 3H), 7.11 (dd, *J* = 8.8 Hz, 8.7 Hz, 4H), 4.26-4.00 (m, 4H), 2.30-0.60 (m, 48H). ^{13}C NMR (125 MHz, $CDCl_3$) δ = 182.6, 161.8, 159.6, 159.5, 158.9, 147.2, 143.8, 136.7, 134.1, 133.8, 131.6, 130.7, 130.5, 129.8, 129.6, 129.5, 128.0, 127.5, 127.3, 127.2, 126.8, 126.4, 125.7, 118.8, 118.4, 117.4, 114.8, 114.8, 110.1, 107.4, 107.4, 95.5, 88.3, 68.2, 37.7, 31.6, 31.6, 29.7, 29.7, 29.3, 25.8, 24.6, 22.7, 22.6, 14.1, 14.0. IR (neat, cm^{-1}): 3303, 3051, 2926, 2856, 2179, 1657, 1604, 1503, 1393, 1369, 1246, 1176, 834. HRMS (ESI) *m/z* calc'd (positive mode) for $C_{62}H_{69}O_3NS_2$ $[M]^+$ 939.4719, found 939.4890.

6-((3,9-bis(2,6-bis(hexyloxy)phenyl)indolizino[6,5,4,3-*ija*]quinolin-5-yl)ethynyl)-4,4-dihexyl-4H-cyclopenta[2,1-*b*:3,4-*b'*]dithiophene-2-carbaldehyde (11b): The synthesis follows the same procedure as 6-((3,9-bis(4-(hexyloxy)phenyl)indolizino[6,5,4,3-*ija*]quinolin-5-yl)ethynyl)-4,4-dihexyl-4H-cyclopenta[2,1-*b*:3,4-*b'*]dithiophene-2-carbaldehyde (**11a**) except 3,9-bis(2,6-bis(hexyloxy)phenyl)-5-ethynylindolizino[6,5,4,3-*ija*]quinoline (**8b**, 55.8 mg) was used in place of 5-ethynyl-3,9-bis(4-(hexyloxy)phenyl)indolizino[6,5,4,3-*ija*]quinoline (**8a**). The crude mixture was purified through silica gel chromatography using 50% dichloromethane:hexanes as the eluent to give a red solid (17.4 mg, 21%). ^{1}H NMR (500 MHz, $CDCl_3$) δ = 9.84 (s,1H), 7.65 (s,1H), 7.61 (d, *J* =8.1 Hz, 1H), 7.56 (s,1H), 7.45-7.29 (m, 3H), 7.21 (s,1H), 7.14 (s,1H), 6.81-6.64 (m, 6H), 4.05-3.90 (m, 8H), 2.00-1.80 (m, 4H), 1.70-0.79 (m, 54H), 0.79-0.61 (m, 12H). ^{13}C NMR (125 MHz, $CDCl_3$) δ = 182.5, 161.8, 158.7, 158.2, 158.1, 147.5, 143.5, 136.1, 132.2, 129.8, 129.4, 128.7, 127.6, 127.4, 127.4, 127.1, 126.6, 125.4, 121.2, 120.0, 117.8, 117.0, 116.6, 116.5, 109.2, 106.9, 106.7, 105.4, 105.4, 105.4, 96.4, 87.4, 69.0, 68.9, 54.1, 37.8, 31.6, 31.3, 31.3, 29.4, 28.9, 28.9, 25.6, 25.5, 24.6, , 22.6, 22.4, 22.3, 14.0, 13.0, 13.8. IR (neat, cm^{-1}): 3367, 3063, 2923, 2851, 1656, 1592, 1496, 1458, 1421, 1395, 1364, 1302, 1247, 1098. HRMS (ESI) *m/z* calc'd (positive mode) for $C_{74}H_{93}O_5NS_2Cs$ $[M+Cs]^+$ 1272.5550, found 1272.5785.

6-((3,9-bis(4-(hexyloxy)phenyl)indolizino[6,5,4,3-*ija*]quinolin-4-yl)ethynyl)-4,4-dihexyl-4H-cyclopenta[2,1-*b*:3,4-*b'*]dithiophene-2-carbaldehyde (12a): The synthesis follows the same procedure as 6-((3,9-bis(4-(hexyloxy)phenyl)indolizino[6,5,4,3-*ija*]quinolin-5-yl)ethynyl)-4,4-dihexyl-4H-cyclopenta[2,1-*b*:3,4-*b'*]dithiophene-2-carbaldehyde (**11a**) only 4-ethynyl-3,9-bis(4-(hexyloxy)phenyl)indolizino[6,5,4,3-*ija*]quinoline (**9a**, 41.3 mg) was used in place of 5-ethynyl-3,9-bis(4-(hexyloxy)phenyl)indolizino[6,5,4,3-*ija*]quinoline (**8a**). The crude mixture was purified through silica gel chromatography using 10% acetone: hexane as the eluent to give a red solid (39 mg, 57%). ^{1}H NMR (500 MHz, $CDCl_3$) δ = 9.88 (s, 1H), 7.96 (br t, 1H), 7.81 (d, *J* = 8.5 Hz, 2H), 7.74 (d, *J* = 8.4 Hz, 2H), 7.62-7.52 (m, 3H), 7.32 (s, 1H), 7.18-6.97 (m, 6H), 7.00 (d, *J* = 4.1 Hz, 1H), 4.13 (t, *J* = 6.4 Hz, 2H), 4.07 (t, *J* = 6.5 Hz, 2H), 2.00-1.80 (m, 8H), 1.69-1.49 (m, 8H), 1.49-0.89 (m, 21H), 0.86 (t, *J* = 6.8 Hz, 12H). ^{13}C NMR (125 MHz, $CDCl_3$) δ = 182.6, 161.8, 159.5, 159.4, 158.9, 147.1, 143.7, 136.9, 136.4, 132.8, 131.6, 131.2, 130.5, 129.8, 129.3, 128.9, 128.1, 127.9, 127.3, 125.8, 125.5, 124.6, 124.1, 120.0, 119.7, 118.7,114.8, 114.2, 109.4, 109.0, 107.3, 94.5, 91.6, 68.2, 68.2, 37.7, 32.0, 31.7, 31.6, 31.6, 31.6, 29.7, 29.6, 29.4, 29.3, 29.2, 25.8, 25.8, 24.6, 22.7, 22.7, 22.7, 22.6, 22.6, 14.1, 14.1, 14.0, 14.0. IR (neat, cm^{-1}): 3020, 2925, 2855, 2362, 2335, 1651, 1504, 1463, 1395, 1362, 1260, 1175, 1023, 892. HRMS (ESI) *m/z* calc'd (positive mode) for $C_{62}H_{69}O_3NS_2Cs$ $[M + Cs]^+$ 1072.3773, found 1072.3646.

6-((3,9-bis(2,6-bis(hexyloxy)phenyl)indolizino[6,5,4,3-*ija*]quinolin-4-yl)ethynyl)-4,4-dihexyl-4H-cyclopenta[2,1-*b*:3,4-*b'*]dithiophene-2-carbaldehyde (12b): To a flame dried, N_2 filled round bottom flask was added 6-bromo-4,4-dihexyl-4H-cyclopenta[2,1-*b*:3,4-*b'*]dithiophene-2-carbaldehyde (**10**)[11] (34 mg, 0.075 mmol, 1.0 equiv.), $Pd(PPh_3)_4$ (13.9 mg, 0.012 mmol, 0.16 equiv.) and dry N,N-dimethylformamide (10.8 ml, 0.007 M). A separate solution of 3,9-bis(2,6-bis(hexyloxy)phenyl)-4-((tributylstannyl)ethynyl)indolizino[6,5,4,3-*ija*]quinoline (**13b**) (158 mg, 0.15 mmol, 2.0 equiv.) in dry *N,N*-dimethylformamide (2.5 ml, 0.06 M) was added dropwise followed with stirring at 110°C and the mixture was stirred overnight. The reaction was cooled down to room temperature and

extracted with diethylether and H_2O. The crude product was further purified by silica column chromatography with 10% ethyl acetate:hexanes to give a red solid (39 mg, 46%). ^{1}H NMR (300 MHz, $CDCl_3$) δ = 9.85 (s, 1H), 7.57 (s, 1H), 7.51-7.41 (m, 3H), 7.36 (dd, *J* = 9.1 Hz, *J* = 8.5 Hz, 2H), 7.23 (s, 1H), 7.19 (s, 1H), 6.72 (d, *J* = 8.2 Hz, 2H), 6.71 (d, *J* = 8.4 Hz, 2H), 6.67 (d, *J* = 4.7 Hz, 1H), 6.67 (d, *J* = 4.7 Hz, 1H), 4.10-3.79 (m, 8H), 2.00-1.75 (m, 4H), 1.75-1.42 (m, 8H), 1.42-0.80 (m, 46H), 0.80-0.60 (m, 12H). ^{13}C NMR (125 MHz, $CDCl_3$) δ = 182.4, 161.6, 158.5, 158.5, 158.3, 158.2, 158.2, 147.9, 143.0, 135.0, 132.4, 129.8, 129.6, 129.4, 127.9, 126.8, 126.6, 126.0, 125.4, 123.8, 123.6, 122.5, 119.6, 119.4, 116.2, 116.0, 109.0, 105.5, 105.5, 105.2, 105.2, 99.6, 93.6, 85.0, 68.9, 68.9, 37.7, 31.7, 31.3, 31.3, 29.7, 29.7, 29.0, 25.6, 25.5, 24.6, 22.6, 22.5, 22.4, 14.0, 13.9, 13.9. IR (neat, cm^{-1}): 3311, 3052, 2926, 2857, 1655, 1590, 1495, 1458, 1421, 1396, 1300, 1228, 1120, 1098, 870.6. HRMS (ESI) *m/z* calc'd (positive mode) for $C_{74}H_{93}O_5NS_2$ $[M]^+$ 1139.6495, found 1139.6481.

3,9-bis(2,6-bis(hexyloxy)phenyl)-4-((tributylstannyl)ethynyl)indolizino[6,5,4,3-*ija*]quinoline (13b): To a N_2 filled flame dried round bottom flask was added 3,9-bis(2,6-bis(hexyloxy)phenyl)-4-ethynylindolizino[6,5,4,3-*ija*]quinoline (**9b**) (100 mg, 0.13 mmol, 1.0 equiv.) and dry THF (4.4 ml, 0.03M). The solution was cooled to -78°C, then 2.5 M *n*-BuLi in hexane (0.06 ml, 0.15 mmol, 1.16 equiv.) was added at -78°C and stirred for 2.5 hours. Bu_3SnCl (0.04 ml, 0.14 mmol, 1.1 equiv.) was added and the whole reaction was stirred at room temperature for 2.5 hours. The reaction mixture was extracted with diethyl ether and H_2O, dried with Na_2SO_4 and evaporated to get the crude product that was used without further purification in the next step (137 mg, 100%). ^{1}H NMR (300 MHz, $CDCl_3$) δ = 7.45-7.24 (m, 5H), 7.10 (d, *J* = 2.7 Hz, 2H), 6.68 (d, *J* =8.4, 2H), 6.65-6.55 (m, 3H), 4.01-3.80 (m, 8H), 1.81-0.80 (m, 59H), 0.80-0.60 (m, 12H).

(*E*)-3-(6-((3,9-bis(4-(hexyloxy)phenyl)indolizino[6,5,4,3-*ija*]quinolin-5-yl)ethynyl)-4,4-dihexyl-4H-cyclopenta[2,1-*b*:3,4-*b'*]dithiophen-2-yl)-2-cyanoacrylic acid (YZ7): To a round bottom flask was added 6-((3,9-bis(4-(hexyloxy)phenyl)indolizino[6,5,4,3-*ija*]quinolin-5-yl)ethynyl)-4,4-dihexyl-4H-cyclopenta[2,1-*b*:3,4-*b'*]dithiophene-2-carbaldehyde (**11a**) (40 mg, 0.04 mmol, 1.0 equiv.) and $CHCl_3$ (0.17 ml). The mixture was degassed with N_2 for 30 minutes, then cyanoacetic acid (11 mg, 0.13 mmol, 3.0 equiv.) and piperidine (0.03 mL, 0.29 mmol, 7.0 equiv.) were added into the flask. The flask was sealed with a plastic stopper and electrical tape and stirred at 90°C for 10 hours. To the reaction mixture was added acetic acid, then the mixture was directly purified through a silica gel plug using first 100% dichloromethane, followed by 10% methanol:90% dichloromethane, and finally 10% methanol:2% acetic acid:88% dichloromethane. Then the dye was again extracted with hexane and water to remove acetic acid and trace silica gel particles. The organic layer was concentrated under reduced pressure to give a purple solid. The product was suspended in hexane solvent then centrifuged five times to give the pure product (43 mg, 97%). ^{1}H NMR (400 MHz, $CDCl_3$/d6-DMSO, 85°C) δ = 8.14 (s, 1H), 7.82 (d, *J* = 8.4 Hz, 2H), 7.77 (d, *J* = 8.4 Hz, 2H), 7.69 (s, 1H), 7.65 (d, *J* = 8.4 Hz, 1H), 7.60-7.55 (m, 2H), 7.44 (d, *J* = 6.4 Hz, 2H), 7.22 (s, 2H), 7.18-7.10 (m, 4H), 4.11 (ap dt, *J* = 6.4, 2.0 Hz, 4H), 1.95-1.90 (m, 4H), 1.81 (ap pent, *J* = 7.2 Hz, 4H), 1.55-1.46 (m, 4H), 1.40-1.36 (m, 8H), 1.18-1.13 (m, 12H), 0.95-0.90 (m, 10H), 0.81 (t, *J* = 6.8 Hz, 6H). ^{13}C NMR spectrum could not be obtained due to the sparing solubility of this dye. IR (neat, cm^{-1}): 3413, 2923, 2854, 2361, 2335, 1600, 1560, 1505, 1366, 1295, 1249, 1174, 1086, 1028, 799. HRMS (ESI) *m/z* calc'd (negative mode) for $C_{65}H_{69}O_4N_2S_2$ $[M-H]^-$ 1005.4699, found 1005.3744. UV-Vis (CH_2Cl_2): λ_{max} = 532 nm (ε = 29,000 M^{-1} cm^{-1}), λ_{onset} = 650 nm. CV (0.1 M Bu_4NPF_6 in CH_2Cl_2, sweep width 2.0-(-1.2.0), 0.1 Vs-1 scan rate) versus NHE: $E_{(S+/S)}$ = 0.90 V; E_g^{opt} = 1.88 eV. $E_{(S+/S^*)}$ = –0.98 V [vs NHE, calculated from $E_{(S+/S^*)} = (E_{(S+/S)} - E_g^{opt})$].

(*E*)-3-(6-((3,9-bis(4-(hexyloxy)phenyl)indolizino[6,5,4,3-*ija*]quinolin-4-yl)ethynyl)-4,4-dihexyl-4H-cyclopenta[2,1-*b*:3,4-*b'*]dithiophen-2-yl)-2-cyanoacrylic acid (YZ12): The synthesis follows the same procedure as (*E*)-3-(6-((3,9-bis(4-(hexyloxy)phenyl)indolizino[6,5,4,3-*ija*]quinolin-5-yl)ethynyl)-4,4-dihexyl-4H-cyclopenta[2,1-*b*:3,4-*b'*]dithiophen-2-yl)-2-cyanoacrylic acid (**YZ7**) except 6-((3,9-bis(4-(hexyloxy)phenyl)indolizino[6,5,4,3-*ija*]quinolin-4-yl)ethynyl)-4,4-dihexyl-4H-cyclopenta[2,1-*b*:3,4-*b'*]dithiophene-2-carbaldehyde (**12a**, 20.2 mg) was used in place of 6-((3,9-bis(4-(hexyloxy)phenyl)indolizino[6,5,4,3-*ija*]quinolin-5-yl)ethynyl)-4,4-dihexyl-4H-cyclopenta[2,1-*b*:3,4-*b'*]dithiophene-2-carbaldehyde (**11a**). Also, after the silica gel plug filtration, the crude product was further purified by silica gel column chromatography with 60% DCM:10% methanol:30% hexane to give a pure purple solid (6.5 mg, 30%). ^{1}H NMR (400 MHz, d6-DMSO, 85°C) δ = 8.00 (s, 1H), 7.91 (d, *J* = 7.2 Hz, 1H), 7.80-7.72 (m, 4H), 7.66 (t, *J* = 7.6 Hz, 1H), 7.61 (s, 1H), 7.48 (s, 1H), 7.31 (s, 1H), 7.19 (d, *J* = 8.4 Hz, 2H), 7.16-7.11 (m, 3H), 6.95 (d, *J* = 4.4 Hz, 1H), 6.09 (s, 1H), 4.15 (t, *J* = 6.8 Hz, 2H), 4.11-4.09 (t, *J* = 6.8 Hz, 2H), 1.94-1.76 (m, 8H), 1.54-1.48 (m, 4H), 1.48-1.13 (m, 20H), 0.95-0.77 (m, 16H) ^{13}C NMR spectrum could not be obtained due to the sparing solubility of this dye. IR (neat, cm^{-1}): 3400, 2955, 2921, 2852, 2335, 1729, 1580, 1569, 1509, 1461, 1360, 1290, 1254, 1170, 1087, 1019, 797. HRMS (ESI) *m/z* calc'd (negative mode) for $C_{65}H_{69}O_4N_2S_2$ $[M-H]^-$ 1005.4699, found 1005.4708. UV-Vis (CH_2Cl_2): λ_{max} = 543 nm (ε = 28,000 M^{-1} cm^{-1}), λ_{onset} = 690 nm. CV (0.1 M Bu_4NPF_6 in CH_2Cl_2, sweep width 2.0-(-1.2.0), 0.1 Vs-1 scan rate) versus NHE: $E_{(S+/S)}$ = 0.90 V; E_g^{opt} = 1.84 eV. $E_{(S+/S^*)}$ = –0.94 V [vs NHE, calculated from $E_{(S+/S^*)} = (E_{(S+/S)} - E_g^{opt})$].

(*E*)-3-(6-((3,9-bis(2,6-bis(hexyloxy)phenyl)indolizino[6,5,4,3-*ija*]quinolin-5-yl)ethynyl)-4,4-dihexyl-4H-cyclopenta[2,1-*b*:3,4-*b'*]dithiophen-2-yl)-2-cyanoacrylic acid (YZ14): The synthesis follows the same procedure as (*E*)-3-(6-((3,9-bis(4-(hexyloxy)phenyl)indolizino[6,5,4,3-*ija*]quinolin-5-yl)ethynyl)-4,4-dihexyl-4H-cyclopenta[2,1-*b*:3,4-*b'*]dithiophen-2-yl)-2-cyanoacrylic acid (**YZ7**) except 6-((3,9-bis(2,6-bis(hexyloxy)phenyl)indolizino[6,5,4,3-*ija*]quinolin-5-yl)ethynyl)-4,4-dihexyl-4H-cyclopenta[2,1-*b*:3,4-*b'*]dithiophene-2-carbaldehyde (**11b**, 17.0 mg) was used in place of 6-((3,9-bis(4-(hexyloxy)phenyl)indolizino[6,5,4,3-*ija*]quinolin-5-yl)ethynyl)-4,4-dihexyl-4H-cyclopenta[2,1-*b*:3,4-*b'*]dithiophene-2-carbaldehyde (**11a**). Also, after the silica gel plug filtration, the crude product was further purified by reverse phase column (C18 silica) with 80% MeOH:acetonitrile to give a red solid (11 mg, 61%). ^{1}H NMR (300 MHz, d6-DMSO, 40°C) δ = 8.02 (s, 1H), 7.69-7.62 (m, 2H), 7.53 (d, *J* = 7.8 Hz, 1H), 7.49-7.35 (m, 3H), 7.25 (s, 1H), 7.11-7.08 (m, 1H), 6.83 (ap t, *J* = 7.8 Hz, 4H), 6.61-6.50 (m, 2H), 4.00-3.90 (m, 8H), 1.90-1.85 (m, 4H), 1.50-0.50 (m, 66H). ^{13}C NMR spectrum could not be obtained due to the sparing solubility of this dye. IR (neat, cm^{-1}): 3050, 2922, 2854, 1732, 1605, 1458, 1361, 1254, 1099, 843. HRMS (ESI) *m/z* calc'd (negative mode) for $C_{77}H_{93}O_6N_2S_2$ $[M-H]^+$ 1205.6475, found 1205.6469. UV-Vis (CH_2Cl_2): λ_{max} = 537 nm (ε = 28,000 M^{-1} cm^{-1}), λ_{onset} = 700 nm. CV (0.1 M Bu_4NPF_6 in CH_2Cl_2, sweep width 2.0-(-1.2.0), 0.1 Vs-1 scan rate) versus NHE: $E_{(S+/S)}$ = 0.71 V; E_g^{opt} = 1.79 eV; $E_{(S+/S^*)}$ = -1.08 V [vs NHE, calculated from $E_{(S+/S^*)} = (E_{(S+/S)} - E_g^{opt})$].

(*E*)-3-(6-((3,9-bis(2,6-bis(hexyloxy)phenyl)indolizino[6,5,4,3-*ija*]quinolin-4-yl)ethynyl)-4,4-dihexyl-4H-cyclopenta[2,1-*b*:3,4-*b'*]dithiophen-2-yl)-2-cyanoacrylic acid (YZ15): The synthesis follows the same procedure as (*E*)-3-(6-((3,9-bis(4-(hexyloxy)phenyl)indolizino[6,5,4,3-*ija*]quinolin-5-yl)ethynyl)-4,4-dihexyl-4H-cyclopenta[2,1-*b*:3,4-*b'*]dithiophen-2-yl)-2-cyanoacrylic acid (**YZ7**) except 6-((3,9-bis(2,6-bis(hexyloxy)phenyl)indolizino[6,5,4,3-*ija*]quinolin-4-yl)ethynyl)-4,4-dihexyl-4H-cyclopenta[2,1-*b*:3,4-*b'*]dithiophene-2-carbaldehyde (**12b**, 18.9 mg) was used in place of 6-((3,9-bis(4-(hexyloxy)phenyl)indolizino[6,5,4,3-*ija*]quinolin-5-yl)ethynyl)-4,4-dihexyl-4H-cyclopenta[2,1-*b*:3,4-*b'*]dithiophene-2-carbaldehyde (**11a**). Also, after the silica gel plug filtration, the crude product was further purified by silica gel chromatography with 5% MeOH:35% dichloromethane:60% hexanes to give a red solid (6.2 mg, 31%). ^{1}H NMR (300 MHz, d6-DMSO, 40 °C) δ = 7.64-7.35 (m, 5H), 7.18 (s, 2H), 6.85-6.74 (m, 5H), 6.66 (s, 1H), 6.52 (s, 1H), 6.43 (s, 1H), 3.94 (br s, 8H), 1.90-1.75 (m, 4H), 1.50-0.50 (m, 66H). ^{13}C NMR spectrum could not be obtained due to the sparing solubility of this dye. IR (neat, cm^{-1}): 3025, 2926, 2856, 1588, 1458, 1373, 1290, 1251, 1098, 1019, 869. HRMS (ESI) *m/z* calc'd (negative mode) for $C_{77}H_{93}O_6N_2S_2$ $[M - H]^+$ 1205.6475, found 1205.7507. UV-Vis (CH_2Cl_2): λ_{max} = 549 nm (ε = 26,000 M^{-1} cm^{-1}), λ_{onset} = 690 nm. CV (0.1 M Bu_4NPF_6 in CH_2Cl_2, sweep width 2.0-(-1.2.0), 0.1 Vs-1 scan rate) versus NHE: $E_{(S+/S)}$ = 0.84 V; E_g^{opt} = 1.89 eV; $E_{(S+/S^*)}$ = –1.05 V [vs NHE, calculated from $E_{(S+/S^*)} = (E_{(S+/S)} - E_g^{opt})$].

Acknowledgements

YZ, HC and JHD thank the National Science Foundation for generous support through a CAREER award 1455167. LM, AHL and NIH thank NSF for award OIA-1539035

Keywords: dye-sensitized solar cells • ullazine • panchromatic • dyes • molecular engineering

[1] a) B. O'Regan, M. Grätzel, *Nature* **1991**, *353*, 737-740; b) A. Fakharuddin, R. Jose, T. M. Brown, F. Fabregat-Santiago, J. Bisquert, *Energy Environ. Sci.* **2014**, *7*, 3952-3981; c) S. Zhang, X. Yang, Y. Numata, L. Han, *Energy Environ. Sci.* **2013**, *6*, 1443-1464.

[2] a) P. Brogdon, H. Cheema, J. H. Delcamp, *ChemSusChem* **2017**, DOI: 10.1002/cssc.201701441; b) S. Mathew, A. Yella, P. Gao, R. Humphry-Baker, B. F. Curchod, N. Ashari-Astani, I. Tavernelli, U. Rothlisberger, M. K. Nazeeruddin, M. Grätzel, *Nat. Chem.* **2014**, *6*, 242-247; c) K. Kakiage, Y. Aoyama, T. Yano, K. Oya, J. I. Fujisawa, M. Hanaya, *Chem. Commun.* **2015**, *51*, 15894-15897.

[3] a) A. Dualeh, R. Humphry-Baker, J. H. Delcamp, M. K. Nazeeruddin, M. Grätzel, *Adv. Energy Mater.* **2013**, *3*, 496-504; b) A. J. Huckaba, F. Giordano, L. E. McNamara, K. M. Dreux, N. I. Hammer, G. S. Tschumper, S. M. Zakeeruddin, M. Grätzel, M. K. Nazeeruddin, J. H. Delcamp, *Adv. Energy Mater.* **2015**, *5*, 1401629; c) J. H. Delcamp, A. Yella, T. W. Holcombe, M. K. Nazeeruddin, M. Grätzel, *Angew. Chem. Int. Ed.* **2013**, *52*, 376-380; d) A. J. Huckaba, A. Yella, P. Brogdon, J. Scott Murphy, M. K. Nazeeruddin, M. Grätzel, J. H. Delcamp, *Chem. Commun.* **2016**, *52*, 8424-8427; e) A. J. Huckaba, A. Yella, L. E. McNamara, A. E. Steen, J. S. Murphy, C. A. Carpenter, G. D. Puneky, N. I. Hammer, M. K. Nazeeruddin, M. Grätzel, J. H. Delcamp, *Chem. Eur. J.* **2016**, *22*, 15536-15542.

[4] H. Cheema, A. Peddapuram, R. E. Adams, L. E. McNamara, L. A. Hunt, N. Le, D. L. Watkins, N. I. Hammer, S. R. H., J. H. Delcamp, *J. Org. Chem.* **2017**, *82*, 12038-12049.

[5] A. Mishra, M. K. Fischer, P. Bauerle, *Angew. Chem. Int. Ed.* **2009**, *48*, 2474-2499.

[6] a) S. Mathew, N. A. Astani, B. F. E. Curchod, J. H. Delcamp, M. Marszalek, J. Frey, U. Rothlisberger, M. K. Nazeeruddin, M. Grätzel, *J. Mater. Chem. A* **2016**, *4*, 2332-2339; b) J. Feng, Y. Jiao, W. Ma, M. K. Nazeeruddin, M. Grätzel, S. Meng, *J. Phys. Chem. C* **2013**, *117*, 3772-3778; c) J. Zhou, W. Yang, B. Wang, H. Ren, *Angew. Chem. Int. Ed.* **2012**, *51*, 12293-12297; d) S. Boldt, S. Parpart, A. Villinger, P. Ehlers, P. Langer, *Angew. Chem. Int. Ed.* **2017**, *56*, 4575–4578; e) R. Berger, M. Wagner, X. Feng, K. Müllen, *Chem. Sci.* **2015**, *6*, 436-441; f) N. A. Drigo, S. Paek, A. J. Huckaba, P. A. Schouwink, N. Tabet, M. K. Nazeeruddin, *Chem. Eur. J.* **2017**, *23*, 17209-17212; g) H. Balli, M. Zeller, *Helv. Chim. Acta* **1983**, *66*, 2135-2139; h) K.-i. Kanno, Y. Liu, A. Iesato, K. Nakajima, T. Takahashi, *Org. Lett.* **2005**, *7*, 5453-5456; i) D. Wan, X. Li, R. Jiang, B. Feng, J. Lan, R. Wang, J. You, *Org. Lett.* **2016**, *18*, 2876-2879; j) H. Qiao, Y. Deng, R. Peng, G. Wang, J. Yuan, S. Tan, *RSC Advances* **2016**, *74*, 70046-70055.

[7] P. Brogdon, F. Giordano, G. A. Puneky, A. Dass, S. M. Zakeeruddin, M. K. Nazeeruddin, M. Grätzel, G. S. Tschumper, J. H. Delcamp, *Chem. Eur. J.* **2016**, *22*, 694-703.

[8] a) K. Pei, Y. Wu, H. Li, Z. Geng, H. Tian, W. H. Zhu, *ACS Appl. Mater. Interfaces* **2015**, *7*, 5296-5304; b) K. D. Seo, I. T. Choi, H. K. Kim, *Chem. Eur. J.* **2015**, *21*, 14804-14811; c) B. E. Hardin, H. J. Snaith, M. D. McGehee, *Nature Photon.* **2012**, *6*, 162-169.

[9] J. Liu, D. Zhou, M. Xu, X. Jing, P. Wang, *Energy Environ. Sci.* **2011**, *4*, 3545.

[10] J. H. Delcamp, Y. Shi, J. H. Yum, T. Sajoto, E. Dell'Orto, S. Barlow, M. K. Nazeeruddin, S. R. Marder, M. Grätzel, *Chem. Eur. J.* **2013**, *19*, 1819-1827.

[11] R. Ziessel, A. Sutter, *Synlett* **2014**, *25*, 1466-1472.

[12] M. R. di Nunzio, B. Cohen, S. Pandey, S. Hayse, G. Piani, A. Douhal, *J. Phys. Chem. C* **2014**, *118*, 11365-11376.

[13] F. Dolhem, C. Lièvre, G. Demailly, *Tetrahedron* **2003**, *59*, 155-164.

10.1002/chem.201800030

WILEY-VCH

Entry for the Table of Contents (Please choose one layout)

Layout 1:

FULL PAPER

A series of metal-free ullazine based D-π-A dyes have been designed and synthesized for the first time. These dyes were characterized by UV-Vis-NIR absorption spectroscopy, cyclic voltammetry, and computational analysis, which reveal suitable characteristics for use in DSC devices. A PCE of 5.6% was obtained for the highest performing dye in the series with a good IPCE onset of 800 nm.

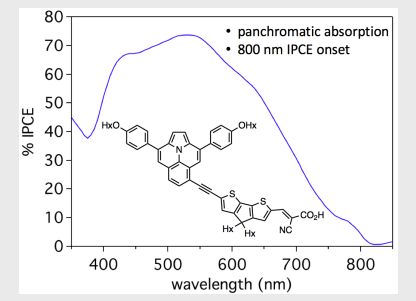

*Yanbing Zhang,[†] Hammad Cheema,[†] Louis McNamara, Leigh Anna Hunt, Nathan I. Hammer, Jared H. Delcamp**

Page No. – Page No.

Ullazine Donor-π bridge-Acceptor Organic Dyes for DSCs